The Energy Source for the Coastal-Trapped Waves in the Australian Coastal Experiment Region

JOHN A. CHURCH AND HOWARD J. FREELAND*

Division of Oceanography, CSIRO Marine Laboratories, Hobart, Tasmania 7001, Australia

(Manuscript received 27 May 1986, in final form 14 August 1986)

ABSTRACT

The sea level on the southern Australian coast is examined for the source of the coastal-trapped wave energy observed during the Australian Coastal Experiment. Sea level, adjusted for atmospheric pressure, and atmospheric pressure are observed to propagate eastward at about 10 m s^{-1}. At the lowest frequency examined (24-day period), some energy travels south along the west coast of Tasmania, but does not reach the east coast of mainland Australia, while some energy travels through Bass Strait to reach the east coast of mainland Australia. At the most energetic frequency (8-day period), adjusted sea levels are coherent over the 3700 km of coastline from southern Australia to the east coast, and much of the wind-forced coastal-trapped wave energy appears to travel through Bass Strait to the mainland east coast. We have not identified a mechanism for energy transfer through Bass Strait, and we do not know what fraction of the coastal-trapped wave energy incident on western Bass Strait actually reaches the east coast. It is suggested that at low frequencies the long wavelength waves are not affected by relatively small gaps in the coastline, but that at higher frequencies the wavelength is smaller and breaks in the coastline become more important. The first and second coastal-trapped wave modes observed at Cape Howe during the Australian Coastal Experiment are most coherent with the sea level at Lakes Entrance at the eastern edge of Bass Strait. It is suggested that these coastal-trapped wave modes are generated when the east–west flow through Bass Strait has to adjust to the narrow shelf of the east Australian coast and that the second mode is preferentially generated because its length scale (k^{-1}) more closely approximates the north–south extent of this east–west flow.

1. Introduction

Theoretical models indicate that coastal-trapped waves (CTWs) are generated by the alongshore component of the wind stress. While a range of modes is generated, the wind is generally more effective at generating the first mode, and it is this mode that has the largest coastal sea-level signal. Also, higher-order modes are preferentially damped by bottom friction. For these reasons, most studies of CTWs have assumed mode 1 is dominant.

Higher-order CTW modes are also thought to be generated by the scattering of the first mode by irregular bottom topography (such as canyons) and major changes in the shelf profile. However, the shelves of western North and South America are of relatively constant width, and generation of higher-order modes by the many canyons on the North American shelf has not been observed.

Most studies of CTWs were completed with datasets gathered for other purposes, and because the instrument arrays did not efficiently determine CTW modal amplitudes, the assumption that the first mode is dominant has generally not been tested. Similarly, the theories that higher-order modes are generated by irregular bottom topography have not been tested. However, Griffin and Middleton (1986) have observed higher-order modes in the lee of an across-shelf barrier.

The Australian Coastal Experiment (ACE), which was completed on the east Australian coast in 1984, showed that a large CTW energy flux was passing Cape Howe, at which point the second-mode CTW was at least as important as the first-mode CTW (Freeland et al., 1986; Church et al., 1986a). These results, which called the assumptions on the dominance of the first mode into doubt, raised two questions: where did the large amount of CTW energy come from? and why was there such an unexpected distribution of energy among the first three modes?

The shelf topography to the south and west of Cape Howe is complicated (Fig. 1); the usual CTW guide is absent, as Bass Strait interrupts its continuity north of the east coast of Tasmania. Further to the west, the CTW guide running along the Great Australian Bight and south to western Tasmania is also interrupted by Bass Strait. (The wave guide is not completely broken, as energy can still travel along the shelf break and slope.) Bass Strait is very shallow (typically 60 to 80 m) compared to the abyssal depths of 4000 to 5000 m in the adjacent ocean. Previous studies of the circulation in Bass Strait have concentrated on the develop-

* Permanent affiliation: Institute of Ocean Sciences, Sidney B.C. V8L 4B2, Canada.

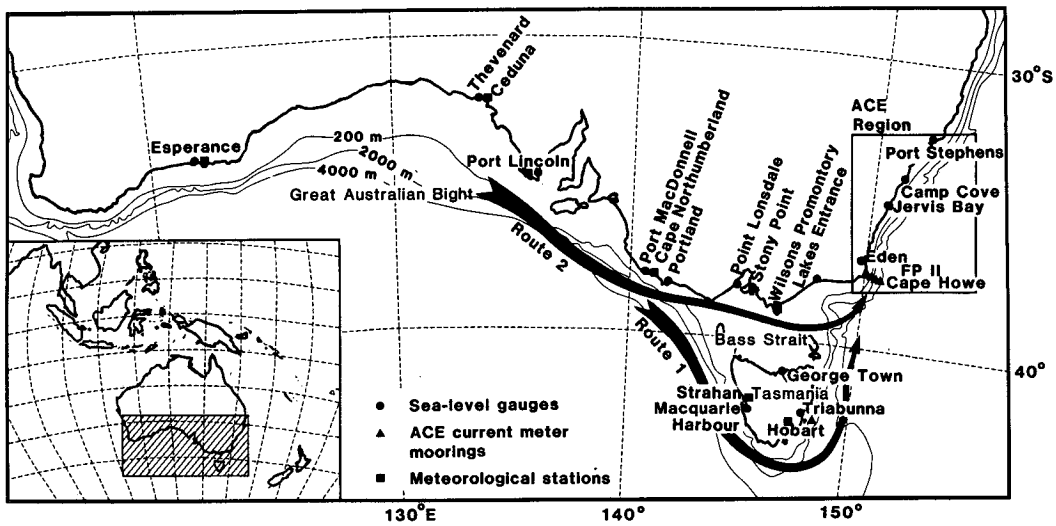

FIG. 1. Location quide. The locations for which coastal sea-level data and atmospheric pressure data were obtained are indicated. The two possible routes for energy to propagate from the Great Australian Bight to the east Australian continental shelf (the ACE region) are also indicated.

ment of numerical models of the tidal (Fandry et al., 1985) and the wind-driven circulations (Fandry, 1982) and on the response to local wind forcing (Jones, 1980). Neither the possible effects of remote forcing nor indications of propagating perturbations have been investigated. This is somewhat surprising in view of the large propagating perturbations in sea level (uncorrected for atmospheric pressure changes) in the Great Australian Bight noted by Krause and Radok (1976) and Provis and Radok (1979).

Two sources for the CTW energy seen on the east Australian coast are examined here. The first is that the alongshelf component of the wind stress drives CTWs in the Great Australian Bight and that these waves propagate across the Bight, south around Tasmania, and then north along the east Australian coast (route 1 on Fig. 1). Alternatively, these CTWs could propagate east to the western entrance of Bass Strait, travel through Bass Strait, and then travel up the east coast (route 2 on Fig. 1). This latter hypothesis has the added attraction that the partition of energy among the modes at Cape Howe would most likely be determined by the frequency of forcing and the geometry of Bass Strait (i.e., when the east–west flow through Bass Strait has to adjust rapidly to the narrow continental shelf of the east coast), rather than by the nature of the waves driving Bass Strait. Hence, in the near field, generation of the second (and higher order) mode CTWs might be expected. Another possibility is that the disturbances are generated solely in the shallow waters of Bass Strait, or on the east coast of Tasmania, and that the disturbances observed in ACE are not correlated with adjusted sea-level perturbations observed in the Great Australian Bight.

The objective of this paper is to look for the source of the CTW energy observed in ACE. A more general question pertinent to this study is the fate of CTWs propagating along a shelf toward a break in the coastline (such as Bass Strait). Are the waves transmitted along the coastline beyond the break? Does the CTW energy pass through the gap, or scatter into higher-order modes? Is the answer to this question dependent on frequency (i.e., on the wavelength in the nondispersive low-frequency limit)? To attempt to shed some light on these questions, we examined sea levels in the Great Australian Bight, in Bass Strait, on the western and eastern coasts of Tasmania, and in the ACE region (Fig. 1). Both the sources of the data used in this study and the method of analysis are outlined in section 2. In section 3, we use the sea-level data (adjusted for atmospheric pressure changes) to look for evidence of propagating CTWs in the Great Australian Bight and to show that these waves are coherent with the CTWs observed during ACE. Spectral techniques are employed to show that for the lowest frequency considered, energy travels via route 2 from the Great Australian Bight to the east coast of mainland Australia and some energy reaches the west coast of Tasmania. However, very little energy appears to reach the ACE region via route 1. At the frequency band containing the most variance (8-day period), we find route 2 is strongly favored. The results and their implications are discussed in section 4.

2. The data

The southern extremity of the main ACE current meter array was opposite Cape Howe (Fig. 1); at this location, data were obtained from current meters on moorings on the 135, 200, 500 and 2000 m isobaths

and from pressure gauges on the 135 and 500 m isobaths. Rather than using the current meter data explicitly, we shall use the amplitude of the first three CTW modes at Cape Howe as determined from observations of alongshore currents by Church et al. (1986a). Full details of the ACE current meter dataset are given in Freeland et al. (1985). We have also used the ACE coastal subsurface pressures (sea level plus atmospheric pressure) for Eden, Jervis Bay, Camp Cove (Sydney), and Port Stephens and a pressure gauge at midshelf at Cape Howe (FP11 in Fig. 1) (see Forbes, 1985, for details of this data). The ACE dataset covers the period early September 1983 until March 1984.

For the present study, additional coastal tide gauge data were collected for Esperance, Thevenard, Port Lincoln, Port MacDonnell, and Portland on the Great Australian Bight; Macquarie Harbour and Triabunna on the western and eastern coasts of Tasmania; and Point Lonsdale, Stony Point, Lakes Entrance, and George Town in Bass Strait. As for the ACE data, the digitized hourly data were low-passed (half-power point at about 40 h) and subsampled at 12 h intervals. Small gaps in the time series of up to 5 days were filled by linear interpolation. The seasonal cycle in the raw data was estimated by fitting a sinusoid with a period of 365.25 days. This signal was then removed from the data before further processing. As the Portland data were virtually identical to the Port MacDonnell data, but with smaller gaps in the series, only the Portland data were used in some of the subsequent analysis. Similarly, the continuous Stony Point data were favored over the more intermittent Point Lonsdale data.

Meteorological data were obtained for a number of standard Bureau of Meteorology stations in the study area. However, of these stations, only stations at Esperance, Ceduna, Port Lincoln, Cape Northumberland, Wilsons Promontory, Strahan, and Hobart recorded atmospheric pressure (once or twice per day). Again, small gaps were filled by linear interpolation and a seasonal cycle was removed.

The additional sea-level and atmospheric pressure data mostly covered the period 1 September 1983 through 31 December 1984. The variances of this data and of the ACE data and the number of valid data points are given in Table 1.

The filtered atmospheric pressure data were added to the filtered sea-level data to give the total subsurface pressure (SSP). The atmospheric pressure data used to correct the filtered sea level are indicated in Table 1. The variances of the adjusted sea levels and the barometer factors are also indicated in Table 1. In determining the confidence intervals, we have assumed that there is one degree of freedom for every 3.5 days of data (3.5 days being the average integral time scale for the data after the seasonal cycle was removed). The barometer factors for the east coast SSP data (Freeland et al., 1986) are also given in Table 1.

For the analysis, we used standard cross-correlations, cross-spectra, and spectral empirical orthogonal functions (EOFs) (Wallace and Dickinson, 1972). In the spectral EOFs, we used the available adjusted sea-level data, but only considered the period for which the ACE data was available (September 1983 to March 1984). Many of the results will be presented as a function of distance from Esperance. The distances of the various locations from Esperance, via both routes discussed in the Introduction (i.e., Bass Strait and southern Tasmania), are presented in Table 2. These distances were estimated by stepping along the coastline and ignoring all bays, gulfs, etc.

TABLE 1. Data statistics. The unadjusted and the adjusted (SSP) sea-level variance, the atmospheric pressure variance, the barometer factor, and the correlation between unadjusted sea level and atmospheric pressure are given. The error bars are the 95% confidence limits and assume an integral time scale of 3.5 days. For the locations in the ACE area (indicated by an *) the results are taken from Freeland et al. (1986).

Sea-level station	Sea-level variance (cm^2)		Total days of adjusted sea level	Meteorological station used	Atmospheric pressure variance (mb^2)	Barometric factor ($cm\ mb^{-1}$)	Correlation
	Unadjusted	Adjusted					
Esperance	173	105	438	Esperance	33	-1.5 ± 0.3	−0.67
Thevenard	330	253	432.5	Ceduna	28	-1.8 ± 0.5	−0.54
Port Lincoln	211	126	458	Port Lincoln	37	-1.6 ± 0.3	−0.69
Port MacDonnell	143	67	328.5	Cape Northumberland	43	-1.2 ± 0.3	−0.72
Portland	126	63	437	Cape Northumberland	43	-1.1 ± 0.2	−0.69
Point Lonsdale	156	73	458.5	Wilsons Promontory	44	-1.4 ± 0.2	−0.76
Stony Point	199	97	481	Wilsons Promontory	44	-1.7 ± 0.2	−0.78
Lakes Entrance	189	167	483.5	Wilsons Promontory	44	-0.7 ± 0.3	−0.36
George Town	88	39	438	Wilsons Promontory	44	-1.1 ± 0.2	−0.75
Macquarie Harbour	285	186	205	Strahan	47	-1.5 ± 0.5	−0.63
Triabunna	136	30	346	Hobart	93	-1.1 ± 0.1	−0.88
*Eden	106	57	205	Eden	31	-1.3 ± 0.4	−0.70
*Jervis Bay	59	55	143	Jervis Bay	30	-0.6 ± 0.5	−0.42
*Camp Cove	72	64	204.5	Camp Cove	28	-0.6 ± 0.5	−0.40
*Port Stephens	71	66	204.5	Port Stephens	25	-0.6 ± 0.5	−0.37

TABLE 2. Distances along the coast from Esperance. The distances are given via the southern Tasmania continental shelf and via Bass Strait.

Route 1: via southern Tasmania		Route 2: via Bass Strait	
Location	Distance (km)	Location	Distance (km)
Esperance	0	Esperance	0
Thevenard	1180	Thevenard	1180
Port Lincoln	1570	Port Lincoln	1570
Port MacDonnell	2140	Port MacDonnell	2140
Portland	2230	Portland	2230
Macquarie Harbour	2780	Point Lonsdale	2530
Triabunna	3200	Stony Point	2590
Lakes Entrance	3720	Lakes Entrance	2920
Eden	3940	Eden	3150
Jervis Bay	4110	Jervis Bay	3320
Camp Cove (Sydney)	4252	Camp Cove (Sydney)	3460
Port Stephens	4452	Port Stephens	3660

3. Results

The barometer factors (the regressions of sea levels on atmospheric pressures—Table 1) for Esperance, Thevenard, Port Lincoln, Point Lonsdale, and Stony Point are significantly above the isostatic value of 1 cm mb^{-1} (i.e., an overresponse to atmospheric pressure perturbations). The barometer factor for Lakes Entrance is not significantly below the isostatic value, but for Camp Cove on the east coast, the value is less than 1 cm mb^{-1}. For stations in the Great Australian Bight, the isostatic model only accounts for a small percentage of the sea-level variance. At Thevenard, for example, only about a quarter of the sea-level variance is explained by an isostatic response. There is a large variance in the SSP for all locations in the Great Australian Bight and this variance is largest at Thevenard, where the shelf is widest. In contrast, the variance of SSP at Triabunna and George Town is small and the isostatic model accounts for most of the sea-level variance.

Spectra of the SSP records (Fig. 2) show that the energy levels at George Town and Triabunna are considerably less than for the other locations. At the remaining locations, the energy levels at the lowest frequency considered (24-day period) are about the same (within a factor of about 2). However, the energy levels at a period of 8 days are dramatically different from one location to the next. For the locations in the Great Australian Bight and in Bass Strait, the spectra have a peak at a frequency of 1 cycle/8 days. The spectra of the SSP at Macquarie Harbour, Eden, George Town, and Triabunna do not show this peak. The spectrum of the second mode CTW at Cape Howe is more similar to the spectra for SSP in the Great Australian Bight than to the spectra of SSP at Eden. All of the spectra fall off with increasing frequency, so that most of the variance occurs at periods exceeding 5 days.

The SSP data for a number of locations and the amplitude of the second-mode CTW at Cape Howe are shown in Fig. 3. For clarity, we have chosen to show only the first seven months of the adjusted sea-level data (i.e., the ACE period). Visual inspection of Fig. 3 indicates that the large SSPs in the Great Australian Bight and the amplitude of the second-mode CTW at Cape Howe are all highly correlated. There is, however, an eastward phase propagation (indicated by the sloping lines connecting individual events). Hence, we must explore the possibility that waves generated in the Great Australian Bight are somehow driving the CTWs observed in ACE. The contour plot (Fig. 4) of the lagged cross-correlations of each station against Stony Point clearly indicates an eastward phase propagation of SSP in the Great Australian Bight and a northward phase propagation on the east coast. Linear regressions through the maxima of the cross-correlations indicate that the phase speeds are 10.3 m s^{-1} in the Great Australian Bight and 3.1 m s^{-1} in the ACE region. This latter value is very close to the value of 3.3 m s^{-1} found by Freeland et al. (1986). (These phase

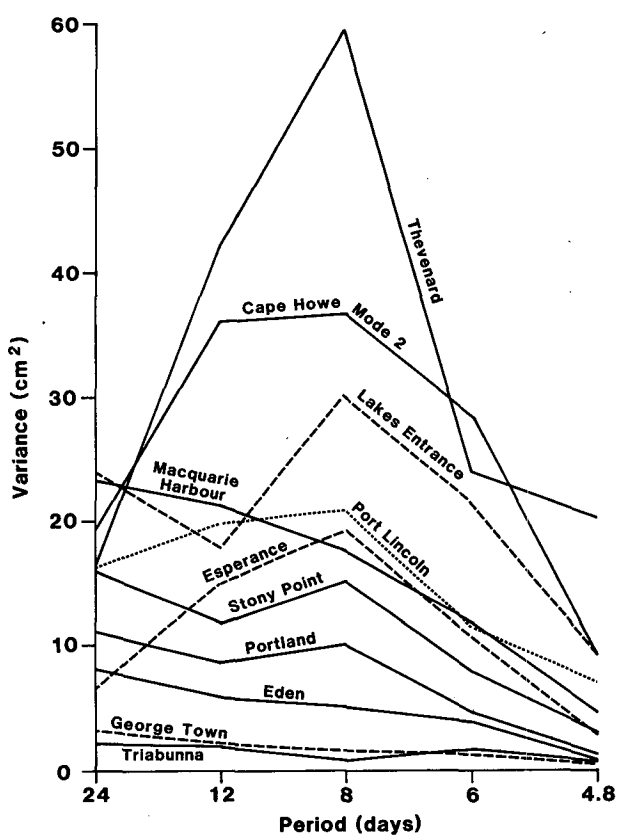

FIG. 2. Spectra of the subsurface pressure data for Esperance, Thevenard, Port Lincoln, Portland, Stony Point, Lakes Entrance, Macquarie Harbour, Triabunna, George Town and Eden. The spectra (arbitrary scale) of the second CTW mode at Cape Howe is also shown. The variance in each frequency band is plotted against frequency on linear scales so that the area under each curve is proportional to the total variance.

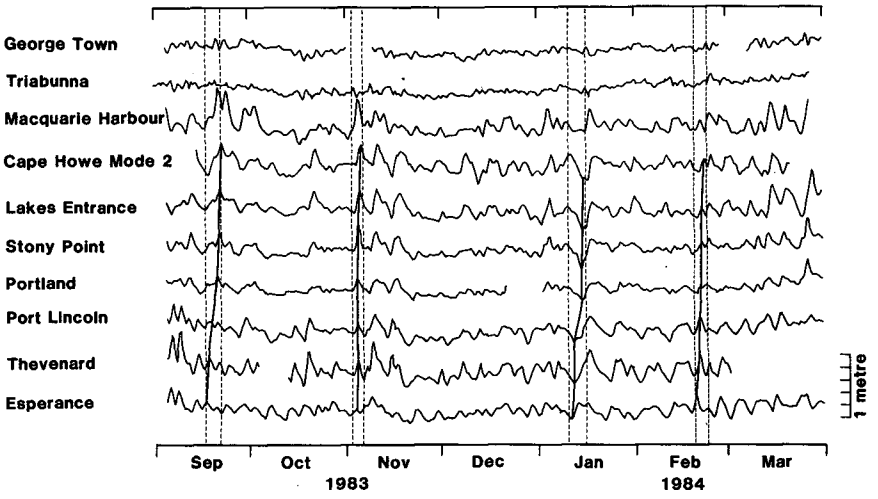

FIG. 3. The subsurface pressure data for Esperance, Thevenard, Port Lincoln, Portland, Stony Point, Lakes Entrance, Macquarie Harbour, Triabunna and George Town. The amplitude (arbitrary scale) of the second CTW mode at Cape Howe is also shown. For clarity, only the first seven months of the data (the ACE period) are shown. The sloping solid lines connect individual events that propagate eastward across southern Australia.

speeds do not agree exactly because in the present analysis all the data were correlated with Stony Point data, whereas Freeland et al. correlated them with Eden data.) These regression lines intersect at the eastern edge of Bass Strait. In drawing Fig. 4, we have assumed that most of the energy passes through Bass Strait en route to the east coast. If instead we assumed that the energy went via the southern Tasmanian continental shelf, the right-hand section of Fig. 4 would be displaced 900 km to the right and an unrealistically fast propagation around southern Tasmania would be implied. Of the locations on the Tasmanian coast, only Macquarie Harbour is significantly correlated with Stony Point.

The first and second CTW modes at Cape Howe are coherent with SSP at Eden and are equally coherent with SSP at Stony Point in Bass Strait and Portland on the western side of Bass Strait. However, the best correlations are between the CTW modes and the SSP on the eastern side of Bass Strait at Lakes Entrance. In all cases, mode 2 is better correlated with the SSP than is mode 1. The maximum correlation of 0.80 is between mode 2 and SSP at Lakes Entrance, with Lakes Entrance leading by 0.4 days.

A similar cross-correlation analysis for the atmospheric pressure data (Fig. 5) gives an eastward propagation speed of 10.4 m s^{-1}. We believe the eastward movement of the atmospheric pressure systems is also reflected in the eastward movement of wind stress on the shelf, but we do not have sufficient high-quality wind data to check this. Forbes (1986) has established that wind stress propagates northward at about 10 m s^{-1} in the ACE region.

The spectral domain analysis has the following frequency band characteristics for one cycle.

1) *24 Days frequency band.* The phases and amplitudes of the first EOF mode (which accounts for 63% of the total variance) are plotted against distance along route 2 in Figs. 6a and 6b. The data for all locations except Jervis Bay are coherent with this EOF mode. The phases indicate an eastward propagation of SSP along the Great Australian Bight at a phase speed of 13.2 m s^{-1} and a northward propagation of 2.7 m s^{-1} on the east Australian coast. The two regression lines through the phases intersect in Bass Strait. The amplitude of the first mode increases from Esperance to Thevenard, then remains fairly constant before a slight decrease in amplitude on the east coast. The amplitude for Macquarie Harbour (plotted as a triangle) is larger than for any other location and is small but not negligible for Triabunna (plotted as a square). The amplitude at George Town (not shown) is 0.14 and lags the Triabunna signal by almost 30°. The phases are consistent with some CTW energy following route 2 through Bass Strait to the east coast of mainland Australia, and they are also consistent with some energy following route 1 to the west and east Tasmanian coast and also to George Town on the north Tasmanian coast. We reject the hypothesis that the Triabunna signal is due to energy passing through Bass Strait and then traveling south (opposite to the propagation direction of CTWs) along the east coast of Tasmania. FP11 and Eden lead Triabunna and Georgetown, and it appears that the energy reaching Triabunna via route 1 does not reach the east coast of mainland Australia.

The second EOF mode accounts for only 23% of the total variance, and only in the Great Australian Bight is there a set of locations coherent with the second EOF mode. The phases indicate an eastward propagation from Esperance to Port Macdonnell.

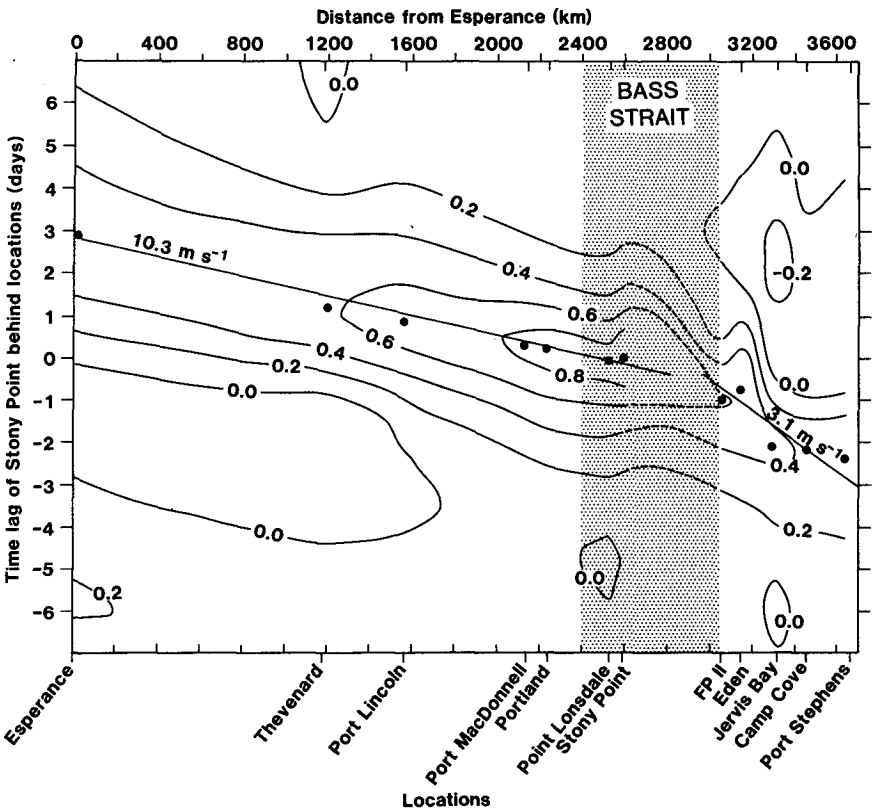

FIG. 4. Contour plot of correlation, for various time lags, of Stony Point with Esperance, Thevenard, Port Lincoln, Port MacDonnell, Portland, Point Lonsdale, Stony Point, FP11, Eden, Jervis Bay, Camp Cove and Port Stephens. The solid dots are the maxima in the correlation functions and the solid lines the least-squares fits to these points for the Great Australian Bight and the east coast. The implied phase speeds are also indicated. In preparing the figure, we assumed that the CTW energy follows route 2 from the Great Australian Bight to the east coast.

Cross-spectra were used to determine the coherence between SSPs along routes 1 and 2. The coherence between SSP at adjacent stations (at the 95% significance level) via both route 2 and route 1 are shown in Fig. 6c and 6d. For route 1 (Fig. 6d), the coherence for adjacent stations pairs, except for Macquarie Harbour and Triabunna, is well above the 95% significance level. Between Macquarie Harbour and Triabunna, the coherence falls just below the 95% significance level. For route 2, the coherences between adjacent station pairs are even higher than they are for route 1.

2) *12 Days frequency band.* In this frequency band, the first empirical mode accounts for 76% of the sea-level variance and the data for all locations except Triabunna and George Town are coherent with this EOF mode. The phases (Fig. 7a) indicate an eastward propagation at 7.2 m s^{-1} across the Great Australian Bight and a northward propagation of 2.6 m s^{-1} on the east coast. The amplitude (Fig. 7b) increases from Esperance to Thevenard and then decreases slowly. There is an indication of a local peak in the amplitude within Bass Strait. In contrast to the 24 day period band, the amplitude at Macquarie Harbour (plotted as a triangle) is now comparable to the other locations. The phase is consistent with some energy propagating south to Macquarie Harbour but the coherence is marginal. The amplitudes at both Triabunna and George Town are negligible.

The second EOF mode accounts for only 15% of the total variance and no significant pattern emerges.

The coherences between adjacent stations (Figs. 7c and 7d) now favor route 2 more strongly. Coherences across Bass Strait (Fig. 7c) are just below the 95% significance level; between the western and eastern sides of Tasmania they are well below the 95% significance level.

3) *8 Days frequency band.* This frequency band contains most of the SSP variance in the Great Australian Bight as well as most of the CTW energy propagating past Cape Howe (Fig. 2). The first empirical mode accounts for 58% of the SSP variance, and the data for all locations except Macquarie Harbour, Triabunna, and George Town are coherent with this EOF mode. The phases (Fig. 8a) indicate an eastward prop-

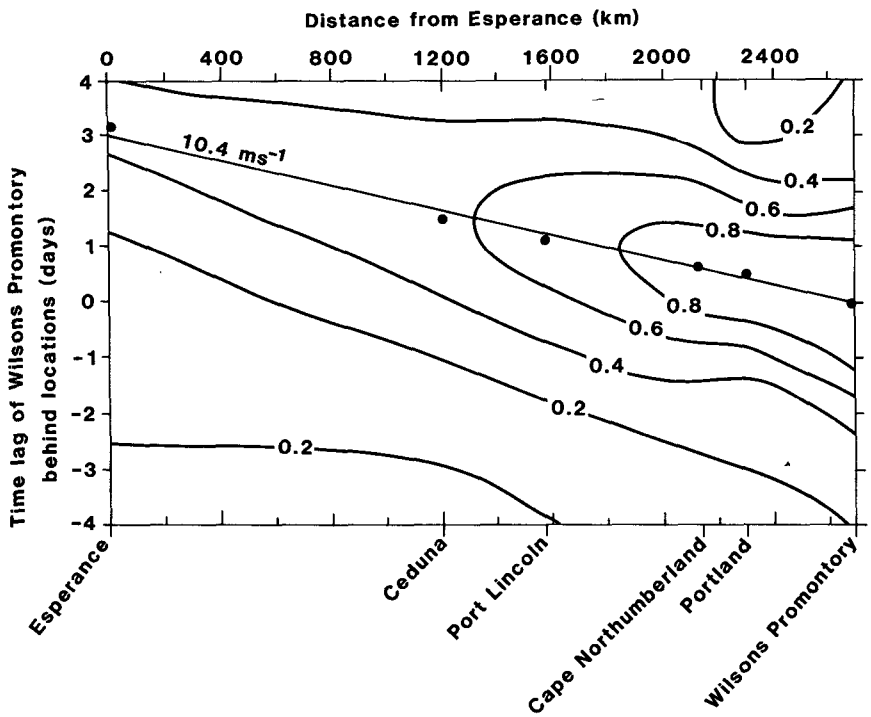

FIG. 5. Contour plot of correlation, for various time lags, of Wilsons Promontory with Esperance, Ceduna, Port Lincoln, Cape Northumberland and Cape Nelson (near Portland). The solid dots are the maxima in the correlation functions and the solid line is the fit to these points. The speed of the eastward phase propagation is also indicated.

agation of 8.3 m s^{-1} and a northward propagation of 3.7 m s^{-1}. The amplitude (Fig. 8b) increases from Esperance to Thevenard and then decreases gradually, but with a peak in Bass Strait. The Macquarie Harbour amplitude and phase are again consistent with some energy propagating south across the western entrance to Bass Strait, but the coherence is not significant. The amplitudes at Triabunna and George Town are negligible.

The second EOF mode accounts for only 23% of the total variance and no significant pattern emerges.

The coherences between adjacent stations again strongly favor route 2 (Fig. 8c). Coherences from the western side to the eastern side of Bass Strait are high, with SSP on the west leading SSP on the east. However, coherences across the western and eastern entrances to Bass Strait are not significant (Fig. 8d). Coherences between the western and eastern sides of Tasmania are just significant at the 95% level.

4) *6 Days frequency band.* This frequency is beyond the maximum in the SSP spectra, and the first empirical mode accounts for 66% of the variance. The data for all locations except Triabunna and George Town are coherent with this EOF mode. The phases (Fig. 9a) indicate an eastward propagation at 14.7 m s^{-1} and a northward propagation at 4.6 m s^{-1}. As for the other frequency bands, the amplitude (Fig. 9b) increases from Esperance to Thevenard and then decreases, but has a pronounced peak in Bass Strait. The Macquarie Harbour amplitude and phase are again consistent with some energy propagating south across the western entrance to Bass Strait, and again the amplitudes at Triabunna and George Town are negligible.

The second EOF mode accounts for only 13% of the total variance, and again no significant pattern emerges.

As for the previous frequency band, the coherences between SSP records (Fig. 9c and 9d) indicate that route 2 is strongly favored. There is a significant coherence between Portland and Macquarie Harbour, but not between Macquarie Harbour and Triabunna or between Triabunna and Lakes Entrance.

4. Discussion

The large barometer factors in the Great Australian Bight (an overresponse of sea level to atmospheric pressure variations) and the large SSP variances indicate that the shelf waters respond dynamically to passing weather systems. The results of the cross-correlation and the spectral empirical orthogonal functions indicate an eastward propagation of SSP at a speed of about 10 m s^{-1}. This speed is about the same speed as the

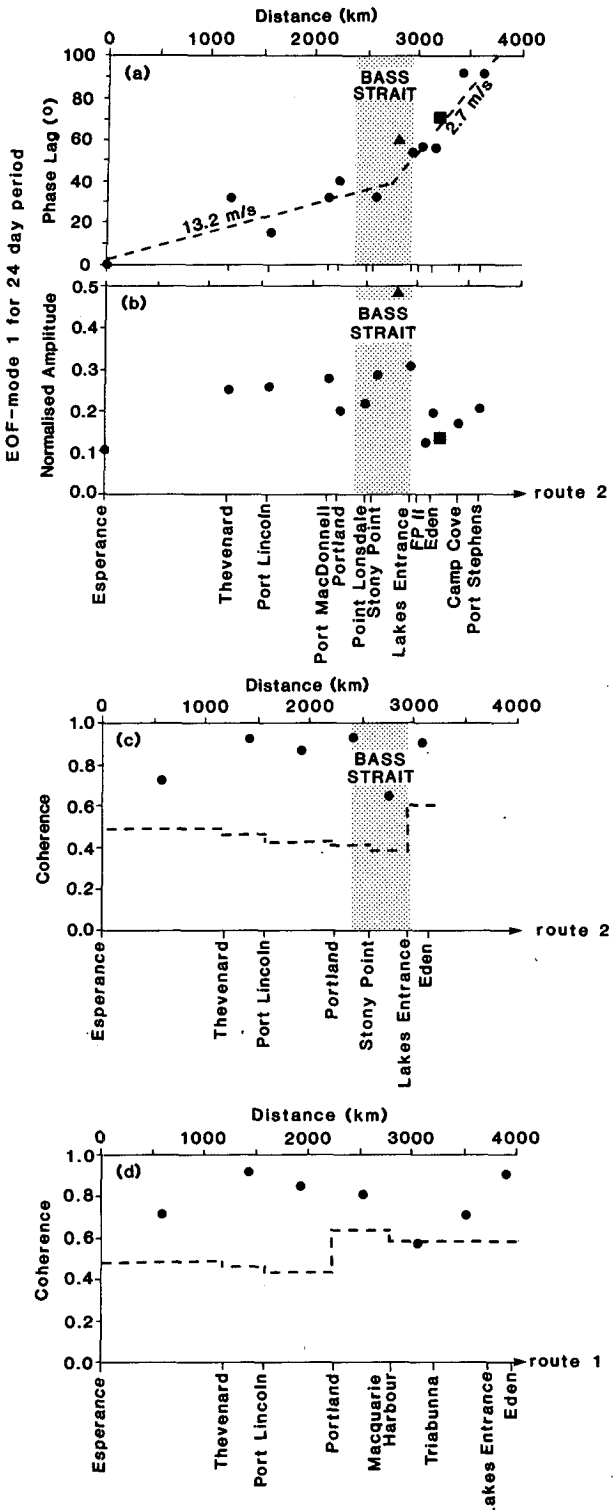

FIG. 6. Frequency domain results for the 24 day period. The phases and amplitudes of the first-mode empirical orthogonal function are shown in (a) and (b). The amplitudes and phases for Macquarie Harbour and Triabunna are plotted as a triangle and a square, respectively. The coherences (and the 95% significance levels) between SSP data along route 2 and route 1 are shown in (c) and (d). Distances in (a), (b) and (c) are via route 2, and in (d) via route 1.

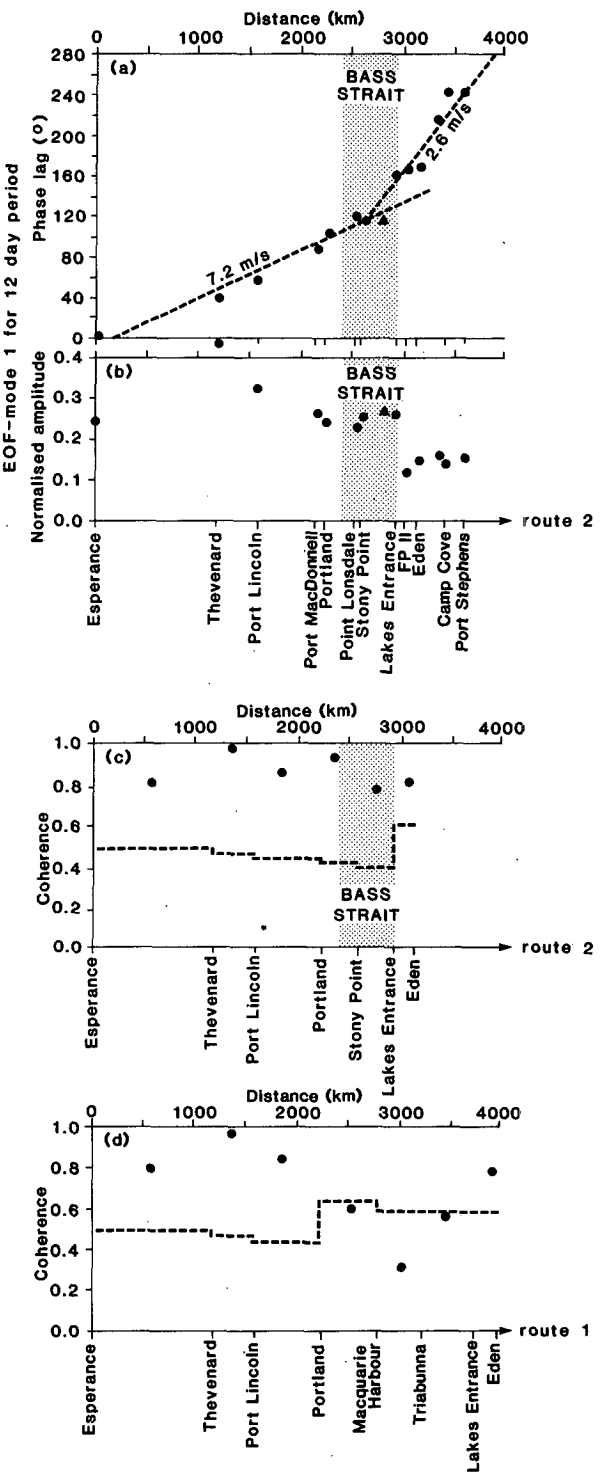

FIG. 7. As in Fig. 6 but for the 12-day period. The amplitudes and phases for Macquarie Harbour are plotted using triangles.

eastward propagation of atmospheric pressure disturbances.

Although the eastward propagation speed appears high, the coastal-trapped wave speed, of order fL, where

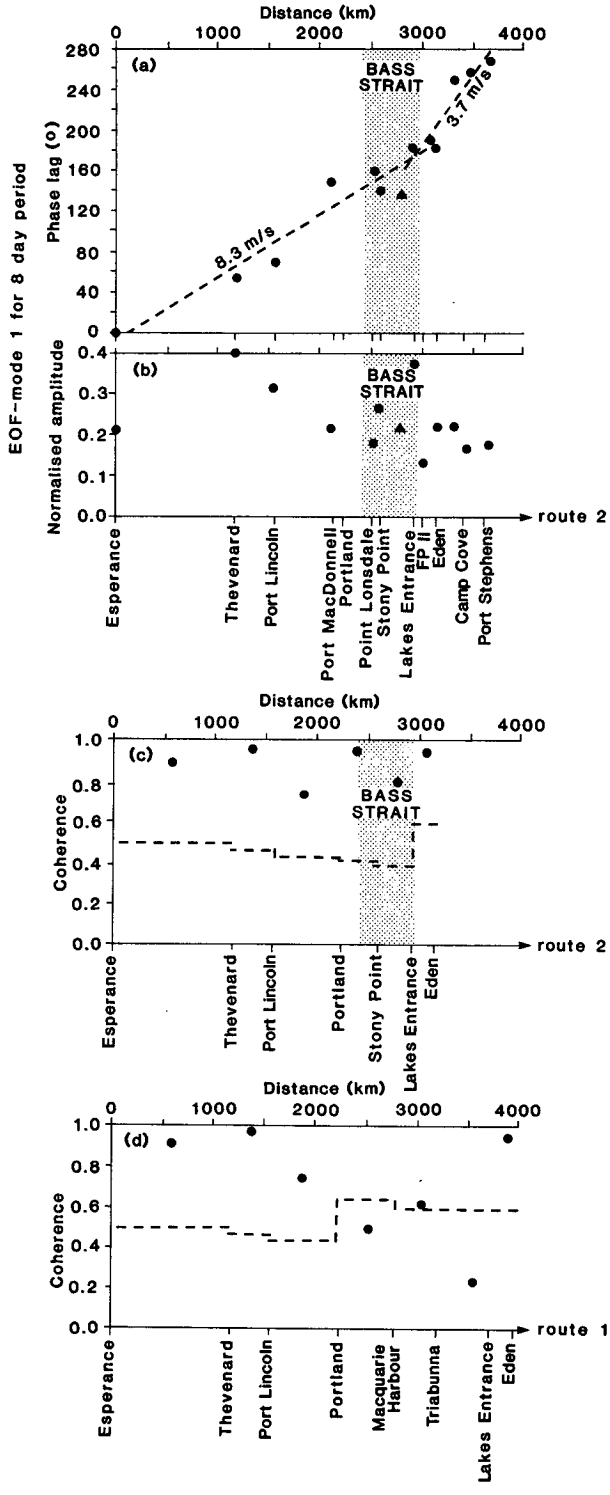

FIG. 8. As in Fig. 7 but for the 8-day period.

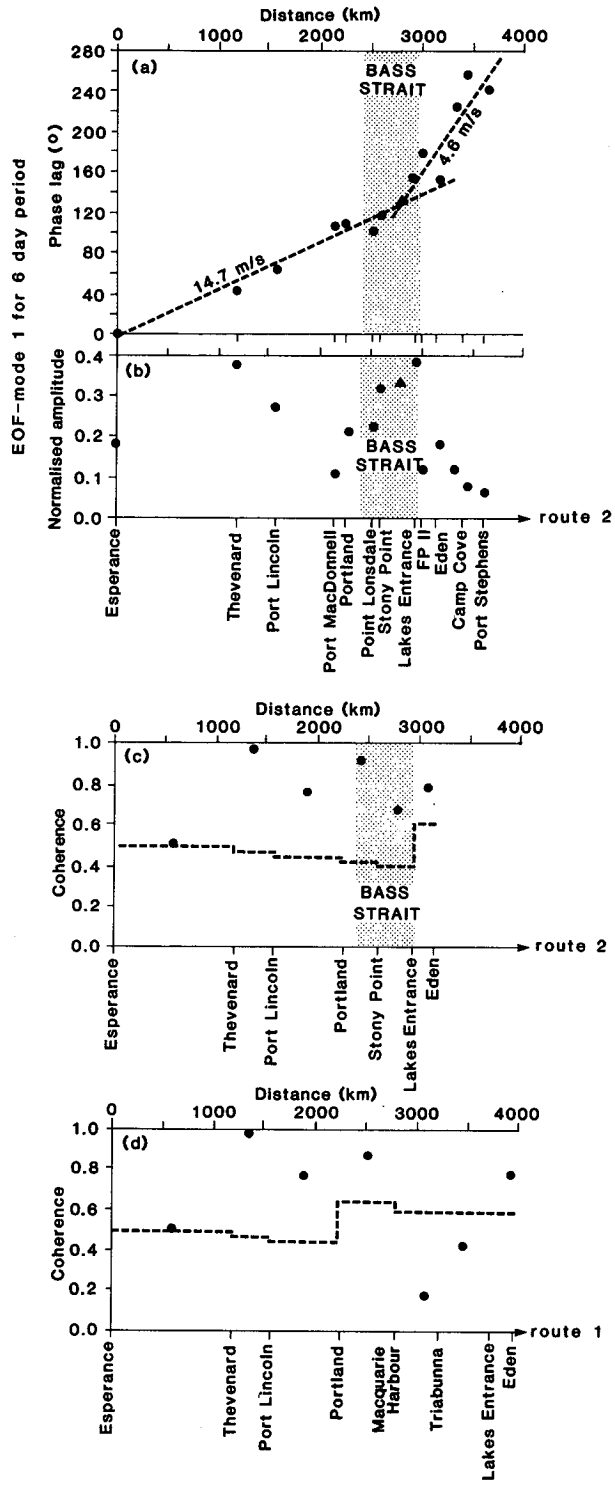

FIG. 9. As in Fig. 7 but for the 6-day period.

f is the Coriolis parameter and L is the shelf width, is also high. For the very wide shelf (about 190 km) offshore from Thevenard, this formula gives 15 m s^{-1}. A more accurate computation of the free wave speed, using the technique of Brink and Chapman (1985) (including stratification as well as topography), gives a value of 16 m s^{-1} for the first mode CTW.

The most likely explanation of the observations in

the Great Australian Bight is forced coastal-trapped wave theory. The propagation speed of the SSP is slower than 16 m s^{-1} because the shelf is generally narrower than 190 km, because of the combination of a free and forced wave response, and because higher-order modes may also be contributing to the observed response. It would appear that the forcing of coastal-trapped waves in the Great Australian Bight is near resonance.

The results of the analysis of SSP on the east coast are consistent with the results found during ACE and indicate northward propagation of coastal-trapped waves. The central question is how observations in the Great Australian Bight and on the east coast are related. The least-squares regression lines for the phases (Figs. 4, 6a, 7a, 8a and 9a) all meet in Bass Strait and the phases are continuous through Bass Strait.

The variance of SSP at Triabunna and George Town was very low and the data looked like white noise. George Town SSP would be affected by CTWs propagating northward past Triabunna and then westward along the northern side of Tasmania and also by waves propagating east along the northern coast of Bass Strait. The small SSP variance at Triabunna indicates that any CTW signal propagating south from along the west coast of Tasmania, around southern Tasmania, then north along the east coast of Tasmania must be very small. In Bass Strait, the barotropic radius of deformation of about 280 km (assuming a mean depth of 70 m) is about equal to the width of the Strait. Assuming the barotropic deformation radius is an appropriate decay scale, the variance at George Town due to waves propagating eastward on the northern coast of Bass Strait would be about one-tenth of that at Stony Point and Lakes Entrance.

At the lowest frequency considered (period of 24 days), the SSP variance at Macquarie Harbour and the results presented in Fig. 5 indicate that some CTW energy is propagating south from the Great Australian Bight to the west coast of Tasmania. Some of this energy does appear to reach Triabunna on the Tasmanian east coast but does not reach the east coast of mainland Australia. However, despite the larger variances in the Great Australian Bight in the 8-day frequency band, there does not seem to be significant energy transfer from the Great Australian Bight to western Tasmania. It appears that at the higher frequencies the CTWs are not as easily able to cross the western entrance into Bass Strait, whereas at the lower frequencies at least some fraction of the energy does make it across the entrance to Bass Strait. The shelf width to the immediate north and south of Bass Strait is about 45 km. The CTW phase speed (fL) is estimated to be about 4.3 m s^{-1}. If k is the alongshore wave number and W the width of the western entrance of Bass Strait, the nondimensional ratio $1/kW$ is about 2 for a period of 8 days, but about 6 for a period of 24 days. Whether or not energy passes across a break in a coastline may depend on the nondimensional number $1/kW$; if the wavelength is large, relatively small gaps in the coastline may not be a significant sink for CTW energy, whereas if the wavelength is smaller, the relatively large gaps may be a significant sink for CTW energy. Further theoretical and numerical work is required to explore this possibility. However, in contrast to the above suggestion, the SSP signals at Portland and Macquarie Harbour are coherent in the 6 day band. We have no explanation for this result except to say that the 6 day period is on the high-frequency tail for the SST spectrum and that there is comparatively little energy at this frequency.

The only observations to the west of Bass Strait available for the present study were coastal sea levels. A significant proportion of the coastal-trapped wave energy is in currents on the continental slope rather than on the shelf. Presumably, this portion of the CTW field is not affected by the break in the coastline as much as are the currents on the shelf, and this energy may continue to propagate along the continental slope. However, we have no observations to pursue this matter and theoretical studies are beyond the scope of the present study. The only current meter observations available to us were those off Cape Howe and on the 200 m isobath off the east coast of Tasmania. The latter showed very low energy levels compared to those at Cape Howe (Freeland et al., 1986) and do not support the concept of significant CTW energy propagating north on the Tasmanian east coast.

Even though the winds to the immediate south of Cape Howe are very strong, CTWs of a magnitude sufficient to explain the ACE observations cannot be generated between the eastern edge of Bass Strait and Cape Howe (Church et al., 1986b). The SSPs on either side of Bass Strait are very coherent, but the SSP at Eden is not particularly coherent with the SSP at Triabunna. Therefore, if most of the CTW energy does not go across the western entrance to Bass Strait, the only remaining path that the energy can follow is through Bass Strait. The phases of the empirical orthogonal function analysis indicate a propagation speed of somewhat less than 15 m s^{-1} from Portland at the western entrance to Bass Strait to Lakes Entrance at the eastern entrance to Bass Strait. However, we do not know of a specific mechanism that agrees with this propagation speed and that would transfer energy through Bass Strait. The barotropic Kelvin wave, the obvious candidate, travels at a speed of $(gh)^{1/2}$. For an average depth in Bass Strait of about 70 m, this speed is about 26 m s^{-1}, faster than the observed propagation speed.

One unexpected result from ACE was that the second-mode CTW carried more energy than the first mode. In the present analysis, we found that mode 2 was more coherent with SSP at Lakes Entrance on the eastern edge of Bass Strait. Here, the east–west flow is confined to flow between the Australian mainland in the north and Flinders Island (Fig. 10) in the south, a

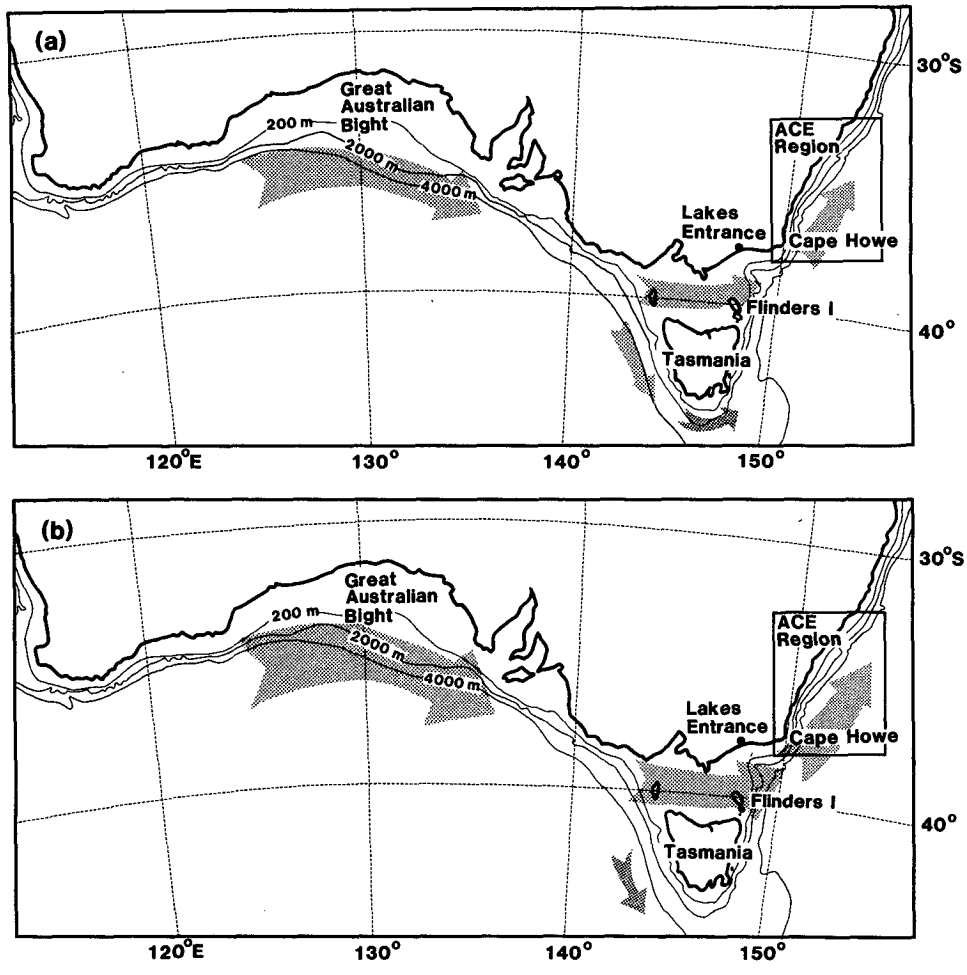

FIG. 10. Schematic diagram of the path of (a) low-frequency (24 day period) and (b) high-frequency (8 day period) CTW energy.

distance of about 200 km. It appears that when this flow has to adjust suddenly to the narrow continental shelf of the east coast, a range of CTW modes is generated. The phase speeds of modes 1 and 2 at Cape Howe (Church et al., 1986a) are 3.2 and 1.8 m s^{-1}, respectively. For a period of 8 days (the peak of the spectra for SSP in the Great Australian Bight and for the CTW modes at Cape Howe), these phase speeds give length scales ($1/k$) of about 350 and 200 km. Mode 2 is likely to be favored because its length scale more closely approximates the north–south extent of the east–west flow at the eastern extremity of Bass Strait. It is interesting to note that theoretical studies presently being undertaken (Buchwald and Kachoyan, personal communication, 1986) also indicated that higher-order CTW modes are generated in models designed to simulate the Bass Strait outflow.

The paths followed by the low- and high-frequency components of the forced CTW energy flux are summarized in Fig. 10. At the lowest frequency considered, energy propagates east from the Great Australian Bight, with some energy passing through Bass Strait and some propagating south to the western coast of Tasmania. However, very little energy appears to get as far as the east coast of Tasmania. At periods of 8 days (the peak of the spectra), adjusted sea levels are coherent over the 3700 km of coastline from Esperance to Port Stephens, and much of the energy propagates from the Great Australian Bight through Bass Strait, generating a number of CTW modes on the east coast. In the Great Australian Bight and in Bass Strait, the CTWs will be near resonantly forced by the eastward-propagating wind systems. Further theoretical and observational studies are needed to elucidate some of the details of the present results. In particular, we have not identified a mechanism for energy transfer through Bass Strait and we do not know what fraction of the CTW energy incident on western Bass Strait actually reaches the east coast.

Acknowledgments. We would like to thank Bernadette Baker for typing this manuscript and Josephine Nunn for drawing the figures. Tidal material for Esperance, Thevenard, Port Lincoln, Port MacDonnell, Portland, Point Lonsdale, George Town, and Stony Point was supplied by the Tidal Laboratory of the Flin-

ders Institute for Atmospheric and Marine Sciences, copyright reserved. Tidal material for Macquarie Harbour was supplied by the Hydro-Electric Commission, Tasmania. We would also like to thank an anonymous referee for a very careful reading of the manuscript and some useful suggestions.

REFERENCES

Brink, K. H., and D. C. Chapman, 1985: Programs for computing properties of coastal-trapped waves and wind-driven motions over the continental shelf and slope. Woods Hole Oceanographic Institute Tech. Rep. WHOI-85-17, 99 pp.

Church, J. A., H. J. Freeland and R. L. Smith, 1986a: Coastal-trapped waves on the east Australian continental shelf. Part I: Propagation of modes. *J. Phys. Oceanogr.*, **16,** 1929–1943.

——, N. J. White, A. J. Clarke, H. J. Freeland and R. L. Smith, 1986b: Coastal-trapped waves on the east Australian continental shelf. Part II: Model verification. *J. Phys. Oceanogr.*, **16,** 1945–1958.

Fandry, C. B., 1982: A numerical model of the wind-driven transient motion in Bass Strait. *J. Geophys. Res.*, **87,** 499–517.

——, G. D. Hubbert and P. C. McIntosh, 1985: Comparison of predictions of a numerical model and observations of tides in Bass Strait. *Aust. J. Mar. Freshwater Res.*, **36,** 737–752.

Forbes, A. M. G., 1985: Sea level data from the Australian Coastal Experiment; a data report. CSIRO Marine Laboratories Rep. No. 170, 16 pp.

Forbes, A. M. G., 1986: Wind-stress in the Australian Coastal Experiment region. *Aust. J. Mar. Freshwater Res.*, **38,** in press.

Freeland, H. J., J. A. Church, R. L. Smith and F. M. Boland, 1985: Current meter data from the Australian Coastal Experiment; a data report. CSIRO Marine Laboratories Rep. No. 169, 51 pp.

——, F. M. Boland, J. A. Church, A. J. Clarke, A. M. G. Forbes, A. Huyer, R. L. Smith, R. O. R. Y. Thompson and N. J. White, 1986: The Australian Coastal Experiment: A search for coastal-trapped waves. *J. Phys. Oceanogr.*, **16,** 1230–1249.

Griffin, D. A., and J. H. Middleton, 1986: Coastal-trapped waves behind a large continental shelf island, Southern Great Barrier Reef. *J. Phys. Oceanogr.*, **16,** 1651–1664.

Jones, I. S. F., 1980: Tidal and wind-driven currents in Bass Strait. *Aust. J. Mar. Freshwater Res.*, **31,** 109–117.

Krause, G., and R. Radok, 1976: Long waves on the southern ocean. *Waves on Water of Variable Depth,* D. G. Provis and R. Radok, Eds., Springer-Verlag, 221–231.

Provis, D. G., and R. Radok, 1979: Sea-level oscillations along the Australian coast. *Aust. J. Mar. Freshwater Res.*, **30,** 295–301.

Wallace, J. M., and R. E. Dickinson, 1972: Empirical orthogonal representation of time series in the frequency domain. Part 1: Theoretical considerations. *J. Appl. Meteor.*, **11,** 887–892.